Inorganic Chemistry

Article

pubs.acs.org/IC

Utilizing 3d–4f Magnetic Interaction to Slow the Magnetic Relaxation of Heterometallic Complexes

Xiao-Lei Li,[†,§] Fan-Yong Min,[†,‡,§] Chao Wang,[†] Shuang-Yan Lin,[†] Zhiliang Liu,*[,‡] and Jinkui Tang*[,†]

[†]State Key Laboratory of Rare Earth Resource Utilization, Changchun Institute of Applied Chemistry, Chinese Academy of Sciences, Changchun 130022, P. R. China

[‡]College of Chemistry and Chemical Engineering, Inner Mongolia University, Hohhot 010021, P. R. China

Supporting Information

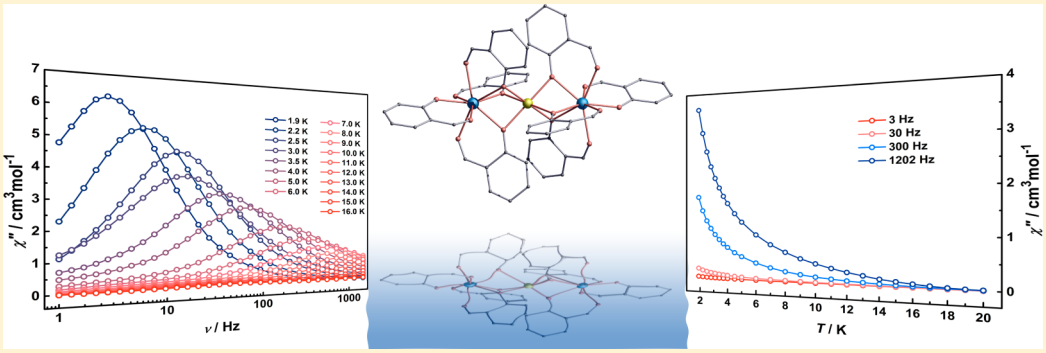

ABSTRACT: The synthesis, structural characterization, and magnetic properties of four related heterometallic complexes with formulas $[Dy^{III}_2Co^{II}(C_7H_5O_2)_8]\cdot 6H_2O$ (**1**), $[Dy^{III}_2Ni^{II}(C_7H_5O_2)_8]\cdot(C_7H_6O_2)_2$ (**2**), $Tb^{III}_2Co^{II}(C_7H_5O_2)_8$ (**3**), and $Dy^{III}_2Cd^{II}(C_7H_5O_2)_8$ (**4**) were reported. Each of complexes has a perfectly linear arrangement of the metal ions with two terminal Ln^{III} (Ln^{III} = Dy^{III}, Tb^{III}) ions and one central M^{II} (M^{II} = Co^{II}, Ni^{II}, Cd^{II}) ion. It was found that **1**–**3** displayed obvious magnetic interactions between the spin carriers according to the direct current (dc) susceptibility measurements. Alternating current (ac) magnetic susceptibility measurements indicate that complexes **1**–**4** all exhibit single-molecule magnet (SMM) behavior, while the replacement of the diamagnetic Cd^{II} by paramagnetic ions leads to a significant slowing of the relaxation thanks to the magnetic interactions between 3d and 4f ions, resulting in higher relaxation barrier for complexes **1** and **2**. Moreover, both Dy_2Co and Dy_2Ni compounds exhibit dual relaxation pathways that may originate from the single ion behavior of individual Dy^{III} ions and the coupling between Dy^{III} and Co^{II}/Ni^{II} ions, respectively, which can be taken as the feature of 3d–4f SMMs. The U_{eff} for **1** of 127 K is a relatively high value among the reported 3d–4f SMMs. The results demonstrate that the magnetic coupling between 3d and 4f ions is crucial to optimize SMM parameters. The synthetic approach illustrated in this work represents an efficient route to design *n*d–4f based SMMs via incorporating suitable paramagnetic 3d and even 4d and 5d ions into the d–f system.

INTRODUCTION

Chemists and physicists have long been sparing no effort to synthesize single-molecule magnets (SMMs) because of their fascinating structures and the possible applications for high-density information storage,[1] molecular spintronic,[2] and quantum computing devices[2c,3] at a molecular level since the discovery of the $Mn_{12}Ac$ cluster, which exhibits slow relaxation of the magnetization behavior, in the 1990s.[4] With the collective aim of obtaining molecules with high-spin ground-state (S_T) and uniaxial (Ising) negative magnetic anisotropy (D), several synthetic strategies can be applied to design new SMMs.[5] Recently it has spurred chemists to focus on not only pure 3d[6] and 4f[5a,c,d,7] metal ions but also the combination of 3d and 4f[8] metal ions since the ferromagnetic coupling between 3d and 4f ions often results in a high-spin ground state, and 3d ions like Co^{II} and Ni^{II} also contribute magnetic anisotropy to the system in conjunction with the large single-ion magnetic anisotropy of 4f ions such as Dy^{III}, Tb^{III}, and so forth.

The first mixed 3d–4f SMM, Cu_2Tb_2, was reported in 2004,[9] while the first Co^{II}–Ln^{III} SMM was a Co^{II}–Gd^{III}–Co^{II} complex reported in 2007.[10] In the next several years, a number of Co^{II}–Ln,[11] Ni^{II}–Ln,[11h,12] and other 3d–4f[13] clusters with diverse structures and nuclearities have been reported to behave as SMMs. It is well-known that the magnetic interactions between the 3d–3d, 3d–4f, and 4f–4f ions in the heterometallic clusters are rather complicated, especially for clusters with high nuclearity. Thus, to better understand the magnetic interactions between 3d–4f metal ions as well as the effect of magnetic interactions on the SMM behavior,[12i,13g] the construction of simple complexes with a limited number of 3d and 4f ions is

Received: January 5, 2015
Published: April 23, 2015

DOI: 10.1021/acs.inorgchem.5b00019
Inorg. Chem. 2015, 54, 4337–4344

Table 1. Crystal Data and Structural Refinement Parameters for 1−4

	1	2	3	4
formula	$C_{56}H_{40}Dy_2CoO_{22}$	$C_{70}H_{52}Dy_2NiO_{20}$	$C_{56}H_{40}Tb_2CoO_{16}$	$C_{56}H_{40}Dy_2CdO_{16}$
F_w (g mol^{-1})	1448.82	1596.81	1345.67	1406.29
cryst syst	monoclinic	monoclinic	monoclinic	triclinic
space group	$P2_1/c$	$P2_1/c$	$P2_1/n$	$P\bar{1}$
T (K)	293(2)	293(2)	293(2)	293(2)
a (Å)	14.913(4)	14.812(2)	10.792(2)	10.024(4)
b (Å)	11.125(3)	10.9693(16)	20.804(4)	11.080(4)
c (Å)	20.084(6)	20.281(3)	11.914(2)	12.217(5)
α [deg]	90	90	90	95.506(7)
β [deg]	108.503(6)	109.248(2)	110.764(3)	113.574(6)
γ [deg]	90	90	90	93.738(7)
V (Å^3)	3159.8(15)	3111.0(8)	2501.1(9)	1229.9(8)
cryst color	yellow	yellow	yellow	yellow
ρ_c (g cm^{-3})	1.523	1.705	1.787	1.899
μ(mm^{-1})	2.671	2.755	3.198	3.510
F(000)	1422	1584	1322	684
R_{int}	0.0743	0.0578	0.0347	0.0280
R [$I > 2\sigma(I)$]	0.0568	0.0430	0.0297	0.0408
wR_2 (all data)	0.1820	0.1171	0.0699	0.0912
GOF	1.029	1.014	1.015	0.995

essential to elucidate the magneto-structural correlations. However, despite Co^{II} and Ni^{II} possessing significant magnetic anisotropy, Co^{II}−Ln and Ni^{II}−Ln SMMs with low-nuclearity are quite sparse[10,11,11d,g,12d,13i,j] and have not received as much attention indeed. Thus, the combination of Co^{II} or Ni^{II} with Ln^{III} ions might present a potential route to design new 3d−4f SMMs.

Recently, we reported a series of new Ln_2Mn heterometallic complexes showing SMM behavior.[14] This result stimulates us to investigate other 3d−4f metal analogues to further explore the effect of magnetic interactions between 3d and 4f ions on the SMM behavior. Accordingly, herein, we report the synthesis, structural characterization, and magnetic behavior of a series of linear 3d−4f heterometallic complexes. Among all complexes exhibiting SMM behavior, the Dy_2Co shows a relatively high energy barrier for 3d−4f SMMs, reaching 127 K. The Dy_2Cd compound with diamagnetic Cd^{II} ion was also investigated to evaluate the effect of the magnetic interactions between the 3d and 4f ions on the SMM behavior. In contrast to the prominent SMM behavior for Dy_2Co, Dy_2Ni, and Dy_2Mn complexes, Dy_2Cd shows relatively lower block temperature, as evidenced by the absence of the out-of-phase alternating current (ac) susceptibility peaks, corroborating that magnetic coupling could suppress tunneling and further enhance the SMM behavior.

EXPERIMENTAL SECTION

General Procedures. All starting materials were of analytical reagent grade and were used as commercially obtained without further purification. *N*-(2-aminopropyl)-2-hydroxybenzamide was prepared according to a procedure previously described in the literature[15] by condensation of phenyl salicylate and 1,2-diaminopropane in a 1:1 molar ratio. All reactions were performed under aerobic conditions. Elemental analyses for C, H, and N were performed on a PerkinElmer 2400 analyzer. IR spectra (4000−300 cm^{-1}) on powdered samples were recorded with a Fourier transform infrared spectrometer nicolet 6700 system, using KBr pellets. All magnetization data were recorded on a Quantum Design MPMS-XL7 SQUID magnetometer equipped with a 7 T magnet. The variable-temperature magnetization was measured with an external magnetic field of 1000 Oe in the temperature range of 2−300 K. The experimental magnetic susceptibilities were corrected for the sample holder and diamagnetism of the constituent atoms, using Pascal's tables.[16]

X-ray Crystallography. Suitable single crystals were selected for single-crystal X-ray diffraction analysis. Crystallographic data were collected at a temperature of 293 K on a Bruker Apex II CCD diffractometer with graphite-monochromated Mo Kα radiation (λ = 0.710 73 Å). Data processing was accomplished with the SAINT processing program. The structure was solved by direct methods and refined on F^2 by full-matrix least-squares using SHELXTL97.[17] The locations of the heaviest metal atoms were easily determined, and the O and C atoms were subsequently determined from the difference Fourier maps. All the non-H atoms were refined anisotropically. The H atoms were introduced in calculated positions and refined with fixed geometry with respect to their carrier atoms. Isotropic treatment was done with the solvent molecules. Additional crystallographic information is available in the Supporting Information.

Synthesis of 1−4. The same procedure was employed to prepare complexes **1**−**4**, and hence only the synthesis of complex **1** will be described here in detail. *N*-(2-aminopropyl)-2-hydroxybenzamide (0.2 mmol) was dissolved in a mixture of methanol and methylene dichloride (1:2, 15 mL), and then salicylic aldehyde (0.2 mmol) was added to the mixture. The reaction mixture was stirred for 5 min. Then, $Co(OAc)_2{\cdot}4H_2O$ (0.2 mmol) and $Dy(NO_3)_3{\cdot}6H_2O$ (0.2 mmol) were added to the above mixture successively; finally, triethylamine (0.1 mmol) was added after 0.5 h. The resulting solution was stirred for another 3 h, followed by filtration, and then was allowed to slowly evaporate without being perturbed. Yellow block single crystals, suitable for X-ray diffraction analysis, were obtained after one week. The crystals were collected by filtration. The analytical data for these complexes are given below. Attempts to isolate analogous compounds with Gd^{III} instead of the anisotropic Tb^{III} and Dy^{III} ions were not successful.

Dy_2Co (1). Yield: 15 mg (41.4% based on salicylic aldehyde). Anal. Calcd for $[Dy^{III}_2Co^{II}(C_7H_5O_2)_8]{\cdot}6H_2O$: C, 46.38; H, 3.59. Found: C, 46.50; H, 3.31%.

Dy_2Ni (2). Yield: 14 mg (43.8% based on salicylic aldehyde). Anal. Calcd for $[Dy^{III}_2Ni^{II}(C_7H_5O_2)_8]{\cdot}(C_7H_6O_2)_2$: C, 52.60; H, 3.25. Found: C, 52.25; H, 3.09%.

Tb_2Co (3). Yield: 20 mg (59.4% based on salicylic aldehyde). Anal. Calcd for $Tb^{III}_2Co^{II}(C_7H_5O_2)_8$: C, 49.93; H, 2.97. Found: C, 49.96; H, 3.08%.

DOI: 10.1021/acs.inorgchem.5b00019
Inorg. Chem. 2015, 54, 4337−4344

Dy_2Cd (4). Yield: 19 mg (54% based on salicylic aldehyde). Anal. Calcd for $Dy^{III}_2Cd^{II}(C_7H_5O_2)_8$: C, 47.78; H, 2.84. Found: C, 47.56; H, 2.79%.

RESULTS AND DISCUSSION

Synthetic Aspects. Complexes **1**−**4** were isolated from the reaction of $M(OAc)_2{\cdot}4H_2O$ (M = Co, Ni, Cd) and $Ln(NO_3)_3{\cdot}6H_2O$ (Ln = Dy, Tb) with *N*-(2-aminopropyl)-2-hydroxybenzamide and salicylic aldehyde[18] in methanol/methylene dichloride (5 mL/10 mL), in the presence of triethylamine. It is worth noting that the *N*-(2-aminopropyl)-2-hydroxybenzamide ligands, although not incorporated in the final structure, may play a crucial role to some extent in the formation of the heterometallic structures since complexes **1**−**4** cannot be obtained without it. Actually, the reaction of *N*-(2-aminopropyl)-2-hydroxybenzamide with salicylaldehyde should give an imine−amide ligand able to coordinate metal ions under aerobic conditions.[19] However, the excess of metal ions and the addition of a small amount of trielthylamine might be unfavorable for the formation of the imine−amide ligand.

Crystal Structures. Single-crystal X-ray diffraction studies indicate that complexes **1** and **2** crystallize in the monoclinic space group $P2_1/c$, whereas complex **4** crystallizes in the triclinic space group $P\bar{1}$ and complex **3** crystallizes in the monoclinic space group $P2_1/n$. The complexes **1**−**4** have similar framework structure, which can be seen from their identical IR spectra (Figure S1, Supporting Information), but there are three H_2O molecules and one salicylic aldehyde molecule in the final structure as the solvent molecules for complexes **1** and **2**, respectively. The structure of **1** will be described as representative of the whole series. Details for the structure solution and refinement are summarized in Table 1. Moreover, for complexes **1** and **4**, the coordination geometry of Dy^{III} ions were calculated by utilizing the SHAPE 2.1 software[20] (Table S1 in Supporting Information). A summary of important selected interatomic distances, the shortest intermolecular distances, and D_{4d} distortion parameters of complexes **1** and **4** are listed in Supporting Information, Table S2.

The partially labeled molecular structure of complex **1** is presented in Figure 1a. As we can see, each ligand utilizes two coordination sites in the formation of **1**, in which eight salicylic aldehyde ligands coordinate with two types of modes: six μ-η^1:η^2 bridging ligands and two chelating ligands (Scheme 1). The molecular structure of complex **1** reveals that the three metal ions are held together via six μ_2-phenolate oxygen atoms of six singly deprotonated salicylic aldehyde ligands according to a concerted coordination action. Each of the terminal Dy^{III} ions and the central Co^{II} ion are bridged by three μ_2-phenolate oxygen atoms to generate a $[Dy_2Co(\mu_2\text{-}O)_6]^{2+}$ core (Figure 1b). Interestingly, the Dy−Co−Dy array in complex **1** is perfectly linear, and a paddle-wheel geometry is seen for **1** when viewed from one end because of this linear arrangement of the three metal ions (Figure 2, right). Three face-sharing polyhedra are generated as a result of the bridging coordination of the phenolate oxygen atoms; furthermore, the symmetrical bridging atoms and three metal ions generate three planes (Figure 2, left and Figure 3a). Each of the two terminal Dy^{III} ions is surrounded by three μ-η^1:η^2 bridging and one chelating salicylic aldehyde ligands and has an overall O_8 coordination environment in a square antiprism (SAP) geometry (Figure 3b, left and middle). The Dy−O bond lengths are in normal ranges of 2.258(7)−2.412(7) Å. The coordination geometry around

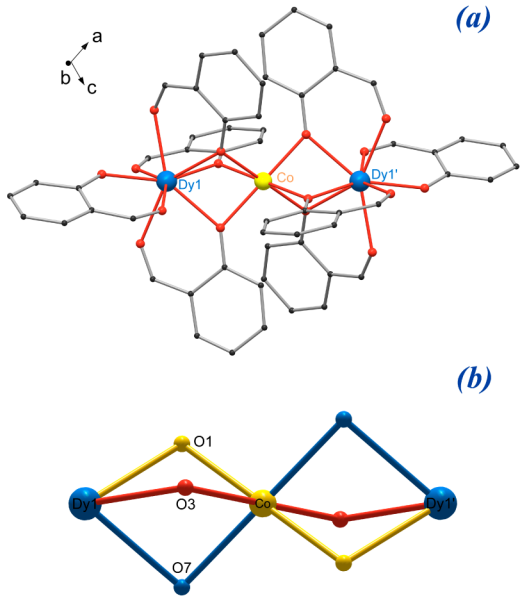

Figure 1. (a) The partially labeled molecular structure of **1**. (b) Core of a Dy_2Co complex in **1**. Hydrogen atoms and H_2O molecules are omitted for clarity. Color scheme: blue, Dy; yellow, Co; red, O; black, C.

Scheme 1. Structure of the Salicylic Aldehyde Ligand and Its Two Specific Coordinate Modes

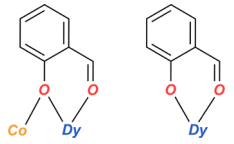

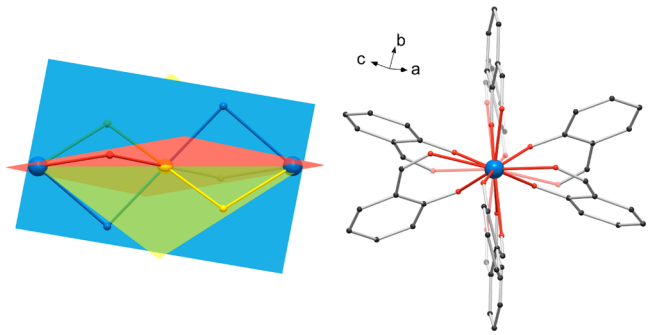

Figure 2. (left) Three planes generated by metal ions and bridging oxygens. (right) The linear arrangement of the metal ions in **1** and overall screw propeller arrangement of the ligand framework around the three metal ions. Unnecessary atoms are omitted for clarity.

the central Co^{II} ion can be described as distorted octahedral with an O_6 donor set with Co−O bond lengths ranging from 2.097(6) Å to 2.149(6) Å (Figure 3b, right). In view of the different space group of **1** and **4**, crystal packing structures along *b* axis of these two complexes are depicted in Figure S2, and careful comparison in the crystallographic distances between **1** and **4** and geometry analysis of the Dy^{III} for them are listed in Tables S1 and S2. From Table S1, we can see that the intermolecular Dy···Dy distance for complex **4** is significantly shorter than that in complex **1**. Thus, the dipolar interactions must be stronger in **4** and may explain the

DOI: 10.1021/acs.inorgchem.5b00019
Inorg. Chem. 2015, 54, 4337−4344

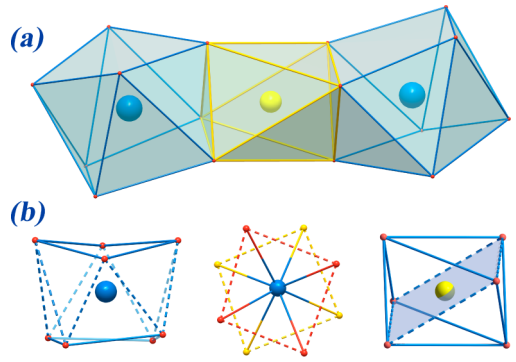

Figure 3. (a) Polyhedral representation of the face sharing successive polyhedra of **1**. (b) Distorted square-antiprism geometry around Dy^{III} ion (left and middle) and distorted octahedron geometry around Co^{II} ion (right).

quantum tunneling of magnetization (QTM) observed (see below).

It is well-known that for a perfect SAP, Φ is 45°, while α corresponds to the magic angle, 54.74°. Wider α angles correspond to compression, and smaller angles correspond to elongation along the tetragonal axis. As shown in Supporting Information, Figure S3 and Table S2, both Dy^{III} ions of **1** and **4** are in SAP geometry, in view of the Dy^{III} coordination sphere; **1** and **4**, obviously, are slightly longitudinally compressed, but with similar α parameters of 58.31 and 57.66°, and the Φ values of 39.56 and 39.44° for **1** and **4**, respectively, indicating that the coordination sphere of two compounds are quite similar.

Magnetic Properties. The direct current (dc) magnetic susceptibility measurements were performed on powdered polycrystalline samples of **1**–**4** in the temperature range of 2–300 K under 1 kOe applied dc field. The product of the molar magnetic susceptibility (χ_M) with temperature versus T plots for **1**–**4** are shown in Figure 4.

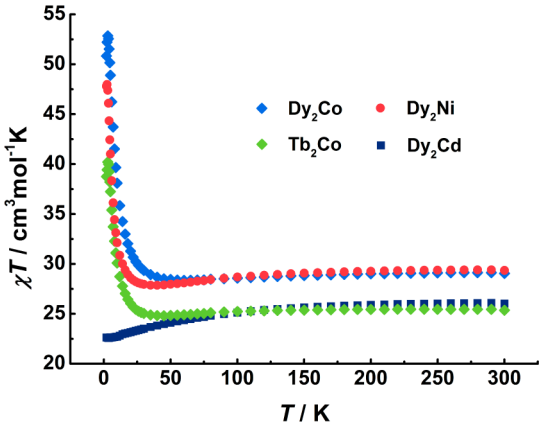

Figure 4. Temperature-dependent χT products under 1000 Oe for **1**–**4**.

The measured room-temperature $\chi_M T$ values for complexes **1**–**3** at 300 K are 29.12, 29.40, and 25.46 cm^3 K mol^{-1}, respectively. These values are in good agreement with the expected values of 30.22, 29.34, and 25.51 cm^3 K mol^{-1} for two noninteracting Dy^{III} (S = 5/2, L = 5, $^6H_{15/2}$, g = 4/3) or Tb^{III} (S = 3, L = 3, $^7H_6$, g = 3/2) ions and one Co^{II} (S = 3/2, $C \approx$ 2.7–3.4 cm^3 K mol^{-1}) or Ni^{II} (S = 1, g = 2) ion as summarized in Table 2.[21] As shown in Figure 4, the dc magnetic properties of

Table 2. Direct Current Magnetic Data for Complexes 1–4

complex	ground state of Ln^{III} ion	$\chi_M T$ expected for noninteracting ions/measured at 300 K/measured at 1.9 K per complex (cm^3 K mol^{-1})	magnetization at 1.9 K and 7 T (μ_B)
1	$^6H_{15/2}$	30.22/29.12/50.83	12.05
2	$^6H_{15/2}$	29.34/29.40/47.80	12.22
3	$^7F_6$	25.51/25.46/38.75	11.78
4	$^6H_{15/2}$	28.34/26.10/22.44	9.51

the complexes **1**–**3** are relatively similar to each other. As the temperature is decreased, the $\chi_M T$ products gradually decrease to 28.36, 27.86, and 24.81 cm^3 K mol^{-1} at ~60, 40, and 45 K, then sharply increase to 52.84, 47.97, and 40.20 cm^3 K mol^{-1} at ~3 K before decreasing again to 1.8 K for complexes **1**–**3**, respectively. The decrease in $\chi_M T$ at higher temperatures for **2** is due to the depopulation of the m_J levels of Dy^{III} ions, whereas for **1** and **3** the decrease can be attributed to both the thermal depopulation of the spin–orbit coupling levels arising from the $^4T_{1g}$ ground term of the octahedral Co^{II} ion and the depopulation of the m_J states of the Dy^{III} and Tb^{III} ions. The sharp increase below 60 K for **1**–**3** indicates obvious ferromagnetic interactions dominating between the spin carriers. The decrease of $\chi_M T$ values in the case of **1**–**3** below 3 K are likely ascribed to the presence of magnetic anisotropies and/or antiferromagnetic intermolecular interactions between the trinuclear complexes.

We now discuss the dc magnetic property of the complex **4**. As shown in Figure 4, at room temperature, the $\chi_M T$ value for complex **4** is 26.10 cm^3 K mol^{-1}, which is slightly lower than the expected value of 28.34 cm^3 mol^{-1} K with the presence of two Dy^{III} (S = 5/2, L = 5, $^6H_{15/2}$, g = 4/3) ions for **4**. Lowering the temperature induces a continuous decrease of the $\chi_M T$ product of **4** to the value 22.44 cm^3 K mol^{-1} at 2 K. This behavior is the expected result[11g] of only depopulation of the Stark sublevels of the Dy^{III} ions for complex **4**.

The field dependence of magnetization M versus H for complexes **1**–**4** was measured between 1.9–5 K (Supporting Information, Figures S4–S7). The magnetization for each of the complexes **1**–**3** below 5 K shows a more abrupt increase below 0.5 T than that of complex **4** confirming the presence of ferromagnetic interactions in these complexes. At higher field the magnetization curves for **1**–**4** follow a linear slope and reach 12.05, 12.22, 11.78, and 9.51 μ_B, respectively, without saturation even up to 7 T. Furthermore, the absence of a superposition of the M versus H/T (Supporting Information, Figures S4–S5, inset figures) data on a single master-curve for **1**–**4** suggesting the presence of significant magnetic anisotropy and/or low-lying excited states in the systems.

The magnetic coupling together with the significant anisotropies of 3d and 4f ions in complexes **1**–**3** is favorable to show SMM behavior. The ac susceptibility measurements were performed under zero dc field for **1**–**4** to investigate the dynamics of the magnetizations. For complex **3**, temperature dependence of the in-phase (χ') and out-of-phase (χ'') ac susceptibility signals under zero external applied dc field exhibit frequency dependence of the χ'' signals below ca. 5 K (Supporting Information, Figures S8–S9), indicating the onset of the slow relaxation of the magnetization. However, no maximum was observed even under 600 Oe external applied dc field, suggesting the presence of fast quantum tunneling relaxation of the magnetization.

DOI: 10.1021/acs.inorgchem.5b00019
Inorg. Chem. 2015, 54, 4337–4344

The strong temperature and frequency dependences of the χ' and χ'' ac susceptibility signals under zero dc field for **1** and **2** (Figures 5 and Supporting Information, Figures S10–S12)

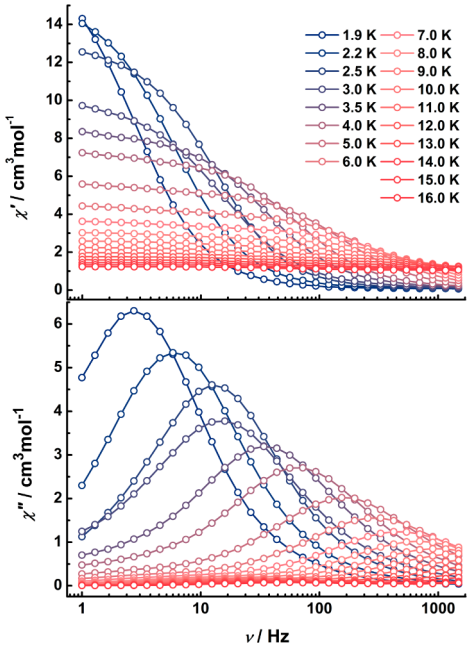

Figure 5. Frequency dependence of the in-phase (χ') and out-of-phase (χ'') ac susceptibility signals for **1** under zero-dc field. The solid lines are a guide for the eyes.

characteristic of SMM behavior are observed, indicating that the introduction of Dy^{III} ion having bistability of ground state and large intrinsic anisotropy are crucial to construct SMMs as compared with complex **3**. As we can see, the Cole–Cole plots in the temperature range of 1.9–16.0 K for **1** exhibited two separate relaxation processes above 5 K, indicating the evolution from faster relaxation (FR) to slower relaxation (SR) as the temperature is raised (Supporting Information, Figures S13–S15), which also can be seen from the frequency dependences of the out-of-phase (χ'') ac susceptibility signals between 10–16 K and is consistent with the overlapping maxima $\chi''(T)$ curves (Supporting Information, Figures S10 and S12). Fitting the diagram at each temperature to a generalized Debye model leads to a parameter α ranging from 0.147 to 0.208 over the temperature range of 1.9–4 K (Supporting Information, Figure S13), while in the 5–13 K range the Cole–Cole plots (Supporting Information, Figures S14 and S15) can be nicely fitted to the sum of two modified Debye functions[22] (eq 1), according to two relaxation processes.

$$\chi_{ac}(\omega) = \chi_{S,tot} + \frac{\Delta\chi_1}{1 + (i\omega\tau_1)^{(1-\alpha_1)}} + \frac{\Delta\chi_2}{1 + (i\omega\tau_2)^{(1-\alpha_2)}} \quad (1)$$

The small parameters α_1 and α_2 (Supporting Information, Table S3) indicate a small distribution of relaxation times for each relaxation process. The relaxation time of **1** was also deduced from the Cole–Cole data between 1.9 and 16 K using generalized Debye model. Modeling the behavior with the Arrhenius law gives two bisecting lines (Figure 6), corresponding to energy barriers (U_{eff}/k_B) of 16.77(4) and 127.27(2) K and pre-exponential factors (τ_0) of 3.55×10^{-5} and 1.69×10^{-9}

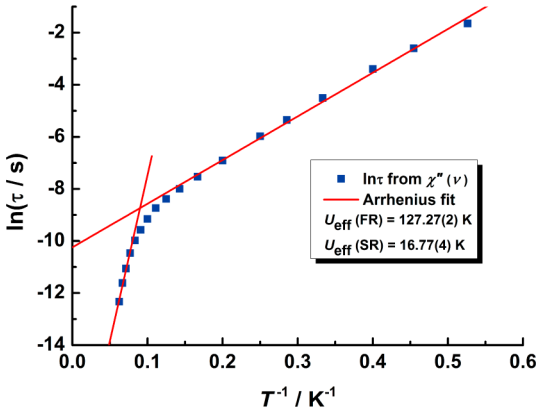

Figure 6. Magnetization relaxation time, $\ln(\tau)$ vs T^{-1} plot for **1** under zero dc field. The solid lines are fitted with the Arrhenius law (see text).

s, below and above 5 K, respectively. At the higher temperature regime the process must be associated with relaxation through excited Kramers doublets of individual Dy^{III} ions, as previously inferred for some Dy complexes,[23] while at low temperatures the weak coupling between Dy^{III} ion and Co^{II} ion might become important, which has been taken as a signature of 3d–4f SMMs.[11b,c] It is worth noting that this U_{eff} for FR is among the high values for 3d–4f SMMs, which is comparable to the $[Mn^{III}{}_6O_3Tb_2]$ and $[Co^{II}{}_2Dy^{III}{}_2]$ cores with U_{eff} of 103 and 118 K, respectively,[11b,24] and lower than that of $[Fe^{II}{}_2Dy^{III}]$ core, which holds the highest energy barrier of 459 K for 3d–4f SMMs.[13g]

Cole–Cole plots (Supporting Information, Figure S16) for **2** under a zero dc field can be nicely fitted by the generalized Debye model for temperatures ranging from 1.9 to 11 K but show moderate relaxation time distribution ($0.20 < \alpha < 0.27$) for temperatures between 1.9 and 5 K. The frequency dependence of the ac susceptibility for complex **2** in an external applied dc field from 100 to 3000 Oe was also measured at 2.5 K (Supporting Information, Figure S17). With increasing field the relaxation rate $1/\tau$ slightly decreases to the highest investigated field of 3000 Oe, indicating partially suppressed QTM. In contrast to the case under zero applied dc field, the frequency-dependent out-of-phase ac susceptibility maxima under 1500 Oe external applied field that vary with frequency are slightly moved to lower frequency (Figure 7). The Cole–Cole plots under 1500 Oe applied static field of complex **2** were also studied in the temperature range of 1.9–12 K (Supporting Information, Figure S18). Fitting the diagram in accordance with one relaxation process for temperatures from 1.9 to 12 K to the generalized Debye model gives parameter α ranging from 0.16 to 0.27. The relatively small values of α parameter for **2** imply that small distribution of relaxation times. The plot of $\ln(\tau)$ versus T^{-1} (Figure 8) shows a crossover at ~5 K, which indicates the presence of dual relaxation processes and hence can be fitted to the Arrhenius law $\tau = \tau_0 \times \exp(U_{eff}/k_BT)$, giving the effective energy barriers of U_{eff} = 12.24 K (pre-exponential factor of $\tau_0 = 1.34 \times 10^{-5}$ s) and U_{eff} = 55.19 K ($\tau_0 = 5.21 \times 10^{-8}$ s) for low- and high-temperature dynamics, respectively. The two relaxation regimes for high and low temperatures can also be associated with single ion behavior of individual Dy^{III} ions and weak coupling between Dy^{III} and Ni^{II} ions, respectively.

DOI: 10.1021/acs.inorgchem.5b00019
Inorg. Chem. 2015, 54, 4337–4344

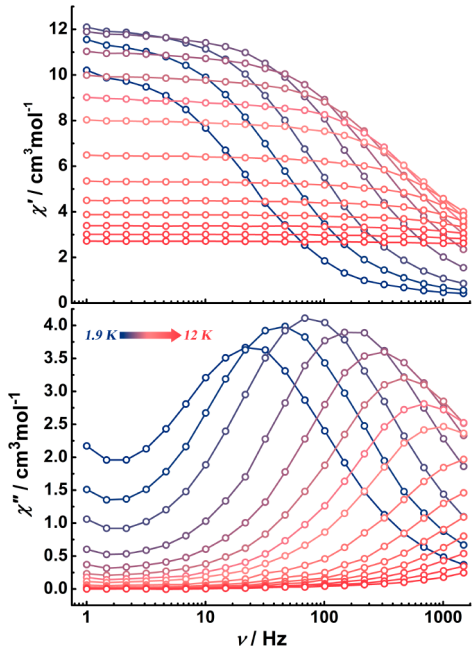

Figure 7. Frequency dependence of the in-phase (χ') and out-of-phase (χ'') ac susceptibility signals for **2** under 1500 Oe. The solid lines are guide for the eyes.

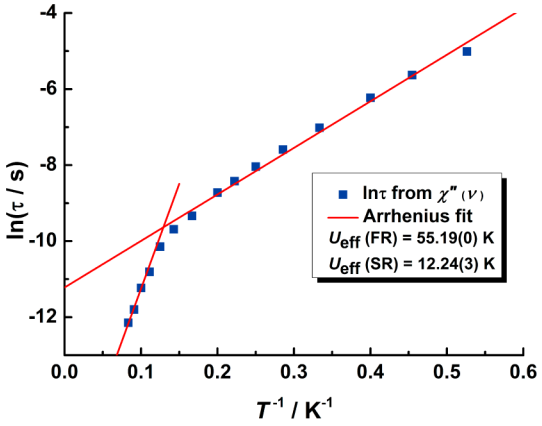

Figure 8. Magnetization relaxation time, $\ln(\tau)$ vs T^{-1} plot for **2** under 1500 Oe. The solid lines are fitted with the Arrhenius law (see text).

The ac susceptibilities of trinuclear Dy_2Cd complex **4** with diamagnetic Cd^{II} of d^{10} electronic configuration were also investigated to evaluate the contribution of magnetic interactions between 3d and 4f ions to the SMM behavior of Dy_2Co, Dy_2Ni and reported Dy_2Mn complexes involving paramagnetic 3d ions. Temperature dependence of the χ' and the χ'' ac susceptibility components are observed below ~18 K under zero dc field for **4**, but without obvious peaks down to 2 K (Supporting Information, Figure S19). Moreover, no peaks of the χ' and the χ'' ac susceptibility components at 1000 Hz and 2.5 K were observed in the field-dependent measurements (Supporting Information, Figure S20), suggesting a lower blocking temperature for complex **4** than that of Dy_2Co and Dy_2Ni complexes. We can see from the ac susceptibility of Dy_2Cd that the magnetic coupling between Dy^{III} and $Co^{II}/Ni^{II}/Mn^{II}$ ions is essential for increasing the blocking temperatures of the Dy_2Co, Dy_2Ni and reported Dy_2Mn heterotrinuclear SMMs.[14] Furthermore, the perfectly linear [Dy^{III}–M^{II}–Dy^{III}] ($M = Co^{II}/Ni^{II}/Mn^{II}$) array might be also responsible for the enhancement of the SMM properties.

In conclusion, four new linear heterometallic Ln–M–Ln complexes have been prepared through the reactions between relevant 3d, 4f metal salts and salicylic aldehyde ligands. The dc magnetic susceptibility measurements show obvious magnetic interactions for complexes **1**–**3**. Complexes **1** and **2** show apparent SMM behavior with a large energy barrier for complex **1**, reaching 127 K. In contrast, the χ'' signals without peaks for complex **4** containing diamagnetic Cd^{II} ion suggest a lower block temperature when compared those of complexes **1** and **2**. The results demonstrate that the magnetic coupling between 3d and 4f ions plays an important role in enhancing SMM behavior. However, it is worth noting that the stronger dipolar interactions in compound **4** as a consequence of the short intermolecular Dy···Dy distance may facilitate fast QTM process. Thus, the magnetic coupling cannot be the only reason for reducing the QTM in complex **1**. The approach illustrated in this work represents a promising strategy to construct efficient *n*d–4f-based SMMs by taking the advantage of strong magnetic interactions between d and f spins through introducing suitable paramagnetic 3d even 4d and 5d ions into the heterometallic d–f system.

■ ASSOCIATED CONTENT

Supporting Information

IR spectra, illustrated crystal packing of complexes **1** and **4**, geometry analysis of **1** and **4**, illustrated coordination polyhedra, selected bond lengths and angles of **1** and **4**, plots of field dependences of magnetization, hysteresis loops, temperature/frequency dependence of ac susceptibility components, Cole–Cole plots, relaxation fitting parameters, crystallographic information in CIF files. This material is available free of charge via the Internet at http://pubs.acs.org. CCDC numbers 1036014 (**1**), 1036015 (**2**), 1036016 (**3**), and 1036018 (**4**) contain supplementary crystallographic data for this paper. These data can be obtained free of charge from the Cambridge Crystallographic Data Centre via www.ccdc.cam.ac.uk/data_request/cif.

■ AUTHOR INFORMATION

Corresponding Authors

*E-mail: tang@ciac.ac.cn. (J.T.)
*E-mail: cezlliu@imu.edu.cn. (Z.L.)

Author Contributions

§Both authors contributed equally to this work.

Notes

The authors declare no competing financial interest.

■ ACKNOWLEDGMENTS

We thank the National Natural Science Foundation of China (Grant Nos. 21371166, 21331003, and 21221061) for financial support.

■ REFERENCES

(1) (a) Sessoli, R.; Gatteschi, D.; Caneschi, A.; Novak, M. A. *Nature* **1993**, *365*, 141–143. (b) Sessoli, R.; Tsai, H. L.; Schake, A. R.; Wang, S.; Vincent, J. B.; Folting, K.; Gatteschi, D.; Christou, G.; Hendrickson, D. N. *J. Am. Chem. Soc.* **1993**, *115*, 1804–1816.

(2) (a) Bogani, L.; Wernsdorfer, W. *Nat. Mater.* **2008**, *7*, 179–186. (b) Friedman, J. R.; Sarachik, M. P.; Tejada, J.; Ziolo, R. *Phys. Rev. Lett.* **1996**, *76*, 3830–3833. (c) Thomas, L.; Lionti, F.; Ballou, R.; Gatteschi, D.; Sessoli, R.; Barbara, B. *Nature* **1996**, *383*, 145–147. (d) Wernsdor-

DOI: 10.1021/acs.inorgchem.5b00019
Inorg. Chem. 2015, 54, 4337–4344

fer, W.; Sessoli, R. *Science* **1999**, *284*, 133−135. (e) Sanvito, S. *Chem. Soc. Rev.* **2011**, *40*, 3336−3355.
(3) (a) Leuenberger, M. N.; Loss, D. *Nature* **2001**, *410*, 789−793. (b) Gatteschi, D.; Sessoli, R. *Angew. Chem., Int. Ed.* **2003**, *42*, 268−297. (c) Aromi, G.; Aguila, D.; Gamez, P.; Luis, F.; Roubeau, O. *Chem. Soc. Rev.* **2012**, *41*, 537−546.
(4) Lis, T. *Acta Crystallogr., Sect. B* **1980**, *36*, 2042−2046.
(5) (a) Sessoli, R.; Powell, A. K. *Coord. Chem. Rev.* **2009**, *253*, 2328−2341. (b) Sorace, L.; Benelli, C.; Gatteschi, D. *Chem. Soc. Rev.* **2011**, *40*, 3092−3104. (c) Zhang, P.; Guo, Y.-N.; Tang, J. *Coord. Chem. Rev.* **2013**, *257*, 1728−1763. (d) Woodruff, D. N.; Winpenny, R. E. P.; Layfield, R. A. *Chem. Rev.* **2013**, *113*, 5110−5148.
(6) (a) Chen, L.; Wang, J.; Wei, J.-M.; Wernsdorfer, W.; Chen, X.-T.; Zhang, Y.-Q.; Song, Y.; Xue, Z.-L. *J. Am. Chem. Soc.* **2014**, *136*, 12213−12216. (b) Poulten, R. C.; Page, M. J.; Algarra, A. G.; Le Roy, J. J.; López, I.; Carter, E.; Llobet, A.; Macgregor, S. A.; Mahon, M. F.; Murphy, D. M.; Murugesu, M.; Whittlesey, M. K. *J. Am. Chem. Soc.* **2013**;. (c) Zadrozny, J. M.; Xiao, D. J.; Atanasov, M.; Long, G. J.; Grandjean, F.; Neese, F.; Long, J. R. *Nat. Chem.* **2013**, *5*, 577−581. (d) Vallejo, J.; Pascual-Álvarez, A.; Cano, J.; Castro, I.; Julve, M.; Lloret, F.; Krzystek, J.; De Munno, G.; Armentano, D.; Wernsdorfer, W.; Ruiz-García, R.; Pardo, E. *Angew. Chem., Int. Ed.* **2013**, *52*, 14075−14079. (e) Saber, M. R.; Dunbar, K. R. *Chem. Commun.* **2014**, *50*, 12266−12269. (f) Boskovic, C.; Brechin, E. K.; Streib, W. E.; Folting, K.; Bollinger, J. C.; Hendrickson, D. N.; Christou, G. *J. Am. Chem. Soc.* **2002**, *124*, 3725−3736. (g) Fortier, S.; Le Roy, J. J.; Chen, C.-H.; Vieru, V.; Murugesu, M.; Chibotaru, L. F.; Mindiola, D. J.; Caulton, K. G. *J. Am. Chem. Soc.* **2013**, *135*, 14670−14678. (h) Freedman, D. E.; Harman, W. H.; Harris, T. D.; Long, G. J.; Chang, C. J.; Long, J. R. *J. Am. Chem. Soc.* **2010**, *132*, 1224−1225. (i) Murrie, M. *Chem. Soc. Rev.* **2010**, *39*, 1986−1995. (j) Kostakis, G. E.; Ako, A. M.; Powell, A. K. *Chem. Soc. Rev.* **2010**, *39*, 2238−2271. (k) Zadrozny, J. M.; Xiao, D. J.; Atanasov, M.; Long, G. J.; Grandjean, F.; Neese, F.; Long, J. R. *Nat. Chem.* **2013**, *5*, 577−581. (l) Zhu, Y.-Y.; Cui, C.; Zhang, Y.-Q.; Jia, J.-H.; Guo, X.; Gao, C.; Qian, K.; Jiang, S.-D.; Wang, B.-W.; Wang, Z.-M.; Gao, S. *Chem. Sci.* **2013**, *4*, 1802−1806. (m) Stamatatos, T. C.; Abboud, K. A.; Wernsdorfer, W.; Christou, G. *Angew. Chem., Int. Ed.* **2008**, *47*, 6694−6698.
(7) (a) Ishikawa, N.; Sugita, M.; Ishikawa, T.; Koshihara, S.; Kaizu, Y. *J. Am. Chem. Soc.* **2003**, *125*, 8694−8695. (b) Ungur, L.; Lin, S.-Y.; Tang, J.; Chibotaru, L. F. *Chem. Soc. Rev.* **2014**, *43*, 6894−6905. (c) Tang, J.; Hewitt, I.; Madhu, N. T.; Chastanet, G.; Wernsdorfer, W.; Anson, C. E.; Benelli, C.; Sessoli, R.; Powell, A. K. *Angew. Chem., Int. Ed.* **2006**, *45*, 1729−1733. (d) Zhang, P.; Zhang, L.; Wang, C.; Xue, S.; Lin, S.-Y.; Tang, J. *J. Am. Chem. Soc.* **2014**, *136*, 4484−4487. (e) Moreno Pineda, E.; Chilton, N. F.; Marx, R.; Dörfel, M.; Sells, D. O.; Neugebauer, P.; Jiang, S.-D.; Collison, D.; van Slageren, J.; McInnes, E. J. L.; Winpenny, R. E. P. *Nat. Commun.* **2014**, *5*, 5243−5249. (f) Wang, Y.-X.; Shi, W.; Li, H.; Song, Y.; Fang, L.; Lan, Y.; Powell, A. K.; Wernsdorfer, W.; Ungur, L.; Chibotaru, L. F.; Shen, M.; Cheng, P. *Chem. Sci.* **2012**, *3*, 3366−3370. (g) Lin, S.-Y.; Wernsdorfer, W.; Ungur, L.; Powell, A. K.; Guo, Y.-N.; Tang, J.; Zhao, L.; Chibotaru, L. F.; Zhang, H.-J. *Angew. Chem., Int. Ed.* **2012**, *51*, 12767−12771. (h) Guo, Y.-N.; Xu, G.-F.; Wernsdorfer, W.; Ungur, L.; Guo, Y.; Tang, J.; Zhang, H.-J.; Chibotaru, L. F.; Powell, A. K. *J. Am. Chem. Soc.* **2011**, *133*, 11948−11951.
(8) (a) Whitehead, G. F. S.; Moro, F.; Timco, G. A.; Wernsdorfer, W.; Teat, S. J.; Winpenny, R. E. P. *Angew. Chem., Int. Ed.* **2013**, *52*, 9932−9935. (b) Novitchi, G.; Pilet, G.; Ungur, L.; Moshchalkov, V. V.; Wernsdorfer, W.; Chibotaru, L. F.; Luneau, D.; Powell, A. K. *Chem. Sci.* **2012**, *3*, 1169−1176. (c) Rinck, J.; Novitchi, G.; Van den Heuvel, W.; Ungur, L.; Lan, Y.; Wernsdorfer, W.; Anson, C. E.; Chibotaru, L. F.; Powell, A. K. *Angew. Chem., Int. Ed.* **2010**, *49*, 7583−7587. (d) Stamatatos, T. C.; Teat, S. J.; Wernsdorfer, W.; Christou, G. *Angew. Chem., Int. Ed.* **2009**, *48*, 521−524.
(9) Osa, S.; Kido, T.; Matsumoto, N.; Re, N.; Pochaba, A.; Mrozinski, J. *J. Am. Chem. Soc.* **2003**, *126*, 420−421.
(10) Chandrasekhar, V.; Pandian, B. M.; Azhakar, R.; Vittal, J. J.; Clérac, R. *Inorg. Chem.* **2007**, *46*, 5140−5142.
(11) (a) Chandrasekhar, V.; Das, S.; Dey, A.; Hossain, S.; Kundu, S.; Colacio, E. *Eur. J. Inorg. Chem.* **2014**, *2014*, 397−406. (b) Mondal, K. C.; Sundt, A.; Lan, Y.; Kostakis, G. E.; Waldmann, O.; Ungur, L.; Chibotaru, L. F.; Anson, C. E.; Powell, A. K. *Angew. Chem., Int. Ed.* **2012**, *51*, 7550−7554. (c) Zou, L.-F.; Zhao, L.; Guo, Y.-N.; Yu, G.-M.; Guo, Y.; Tang, J.; Li, Y.-H. *Chem. Commun.* **2011**, *47*, 8659−8661. (d) Costes, J.-P.; Vendier, L.; Wernsdorfer, W. *Dalton Trans.* **2011**, *40*, 1700−1706. (e) Zhao, X.-Q.; Lan, Y.; Zhao, B.; Cheng, P.; Anson, C. E.; Powell, A. K. *Dalton Trans.* **2010**, *39*, 4911−4917. (f) Abtab, S. M. T.; Majee, M. C.; Maity, M.; Titiš, J.; Boča, R.; Chaudhury, M. *Inorg. Chem.* **2014**, *53*, 1295−1306. (g) Chandrasekhar, V.; Pandian, B. M.; Vittal, J. J.; Clérac, R. *Inorg. Chem.* **2009**, *48*, 1148−1157. (h) Zhao, F.-H.; Li, H.; Che, Y.-X.; Zheng, J.-M.; Vieru, V.; Chibotaru, L. F.; Grandjean, F.; Long, G. J. *Inorg. Chem.* **2014**, *53*, 9785−9799. (i) Langley, S. K.; Chilton, N. F.; Moubaraki, B.; Murray, K. S. *Polyhedron* **2013**, *66*, 48−55.
(12) (a) Chandrasekhar, V.; Pandian, B. M.; Boomishankar, R.; Steiner, A.; Vittal, J. J.; Houri, A.; Clérac, R. *Inorg. Chem.* **2008**, *47*, 4918−4929. (b) Colacio, E.; Ruiz, J.; Mota, A. J.; Palacios, M. A.; Cremades, E.; Ruiz, E.; White, F. J.; Brechin, E. K. *Inorg. Chem.* **2012**, *51*, 5857−5868. (c) Zhao, L.; Wu, J.; Ke, H.; Tang, J. *Inorg. Chem.* **2014**, *53*, 3519−3525. (d) Das, S.; Dey, A.; Kundu, S.; Biswas, S.; Mota, A. J.; Colacio, E.; Chandrasekhar, V. *Chem.—Asian J.* **2014**, *9*, 1876−1887. (e) Chakraborty, A.; Bag, P.; Riviere, E.; Mallah, T.; Chandrasekhar, V. *Dalton Trans.* **2014**, *43*, 8921−8932. (f) Colacio, E.; Ruiz-Sanchez, J.; White, F. J.; Brechin, E. K. *Inorg. Chem.* **2011**, *50*, 7268−7273. (g) Meseguer, C.; Titos-Padilla, S.; Hänninen, M. M.; Navarrete, R.; Mota, A. J.; Evangelisti, M.; Ruiz, J.; Colacio, E. *Inorg. Chem.* **2014**, *53*, 12092−12099. (h) Yamaguchi, T.; Sunatsuki, Y.; Ishida, H.; Kojima, M.; Akashi, H.; Re, N.; Matsumoto, N.; Pochaba, A.; Mroziński, J. *Inorg. Chem.* **2008**, *47*, 5736−5745. (i) Pointillart, F.; Bernot, K.; Sessoli, R.; Gatteschi, D. *Chem.—Eur. J.* **2007**, *13*, 1602−1609. (j) Meng, Z.-S.; Guo, F.-S.; Liu, J.-L.; Leng, J.-D.; Tong, M.-L. *Dalton Trans.* **2012**, *41*, 2320−2329. (k) Goura, J.; Guillaume, R.; Rivière, E.; Chandrasekhar, V. *Inorg. Chem.* **2014**, *53*, 7815−7823. (l) Ke, H.; Zhao, L.; Guo, Y.; Tang, J. *Inorg. Chem.* **2012**, *51*, 2699−2705. (m) Mondal, K. C.; Kostakis, G. E.; Lan, Y.; Wernsdorfer, W.; Anson, C. E.; Powell, A. K. *Inorg. Chem.* **2011**, *50*, 11604−11611.
(13) (a) Ako, A. M.; Mereacre, V.; Clerac, R.; Wernsdorfer, W.; Hewitt, I. J.; Anson, C. E.; Powell, A. K. *Chem. Commun.* **2009**, 544−546. (b) Chilton, N. F.; Langley, S. K.; Moubaraki, B.; Murray, K. S. *Chem. Commun.* **2010**, *46*, 7787−7789. (c) Liu, J.-L.; Guo, F.-S.; Meng, Z.-S.; Zheng, Y.-Z.; Leng, J.-D.; Tong, M.-L.; Ungur, L.; Chibotaru, L. F.; Heroux, K. J.; Hendrickson, D. N. *Chem. Sci.* **2011**, *2*, 1268−1272. (d) Zhang, P.; Zhang, L.; Lin, S.-Y.; Tang, J. *Inorg. Chem.* **2013**, *52*, 6595−6602. (e) Mereacre, V. M.; Ako, A. M.; Clérac, R.; Wernsdorfer, W.; Filoti, G.; Bartolomé, J.; Anson, C. E.; Powell, A. K. *J. Am. Chem. Soc.* **2007**, *129*, 9248−9249. (f) Mori, F.; Nyui, T.; Ishida, T.; Nogami, T.; Choi, K.-Y.; Nojiri, H. *J. Am. Chem. Soc.* **2006**, *128*, 1440−1441. (g) Liu, J.-L.; Wu, J.-Y.; Chen, Y.-C.; Mereacre, V.; Powell, A. K.; Ungur, L.; Chibotaru, L. F.; Chen, X.-M.; Tong, M.-L. *Angew. Chem., Int. Ed.* **2014**, *53*, 12966−12970. (h) Kuhne, I. A.; Magnani, N.; Mereacre, V.; Wernsdorfer, W.; Anson, C. E.; Powell, A. K. *Chem. Commun.* **2014**, *50*, 1882−1885. (i) Towatari, M.; Nishi, K.; Fujinami, T.; Matsumoto, N.; Sunatsuki, Y.; Kojima, M.; Mochida, N.; Ishida, T.; Re, N.; Mrozinski, J. *Inorg. Chem.* **2013**, *52*, 6160−6178. (j) Yamaguchi, T.; Costes, J.-P.; Kishima, Y.; Kojima, M.; Sunatsuki, Y.; Bréfuel, N.; Tuchagues, J.-P.; Vendier, L.; Wernsdorfer, W. *Inorg. Chem.* **2010**, *49*, 9125−9135.
(14) Li, X.-L.; Min, F.-Y.; Wang, C.; Lin, S.-Y.; Liu, Z.; Tang, J. *Dalton Trans.* **2015**, *44*, 3430−3438.
(15) Mitsuhashi, R.; Suzuki, T.; Sunatsuki, Y.; Kojima, M. *Inorg. Chim. Acta* **2013**, *399*, 131−137.
(16) Kahn, O. *Molecular Magnetism;* VCH: New York, 1993.
(17) Sheldrick, G. *Acta Crystallogr., Sect. A* **2008**, *64*, 112−122.
(18) Watanabe, A.; Yamashita, A.; Nakano, M.; Yamamura, T.; Kajiwara, T. *Chem.—Eur. J.* **2011**, *17*, 7428−7432.

DOI: 10.1021/acs.inorgchem.5b00019
Inorg. Chem. 2015, 54, 4337−4344

(19) Costes, J.-P.; Dahan, F.; Donnadieu, B.; Rodriguez Douton, M.-J.; Fernandez Garcia, M.-I.; Bousseksou, A.; Tuchagues, J.-P. *Inorg. Chem.* **2004**, *43*, 2736−2744.
(20) Casanova, D.; Llunell, M.; Alemany, P.; Alvarez, S. *Chem.—Eur. J.* **2005**, *11*, 1479−1494.
(21) Benelli, C.; Gatteschi, D. *Chem. Rev.* **2002**, *102*, 2369−2388.
(22) Guo, Y.-N.; Xu, G.-F.; Guo, Y.; Tang, J. *Dalton Trans.* **2011**, *40*, 9953−9963.
(23) Guo, Y.-N.; Xu, G.-F.; Gamez, P.; Zhao, L.; Lin, S.-Y.; Deng, R.; Tang, J.; Zhang, H.-J. *J. Am. Chem. Soc.* **2010**, *132*, 8538−8539.
(24) Hołyńska, M.; Premužić, D.; Jeon, I.-R.; Wernsdorfer, W.; Clérac, R.; Dehnen, S. *Chem.—Eur. J.* **2011**, *17*, 9605−9610.

DOI: 10.1021/acs.inorgchem.5b00019
Inorg. Chem. 2015, 54, 4337−4344